ARTICLE

doi:10.1016/j.ymthe.2006.07.008

# Preferential Silencing of a Common Dominant Rhodopsin Mutation Does Not Inhibit Retinal Degeneration in a Transgenic Model

Alessandra Tessitore,[1] Fabiana Parisi,[1] Michela Alessandra Denti,[2] Mariacarmela Allocca,[1,3] Umberto Di Vicino,[1] Luciano Domenici,[4,5] Irene Bozzoni,[2] and Alberto Auricchio[1,6,*]

[1]*Telethon Institute of Genetics and Medicine, 80131 Naples, Italy*
[2]*Institute Pasteur Cenci-Bolognetti, Department of Genetics and Molecular Biology, University of Rome La Sapienza and IBPM of CNR, Rome, Italy*
[3]*European School of Molecular Medicine (SEMM), Naples site, Italy*
[4]*Institute of Neuroscience (CNR), 56100 Pisa, Italy*
[5]*Department of Biomedical Sciences and Technology, University of L'Aquila, 67010 L'Aquila, Italy*
[6]*Department of Pediatrics, "Federico II" University, Naples, Italy*

**To whom correspondence and reprint requests should be addressed at the Telethon Institute of Genetics and Medicine, Via P. Castellino, 111, 80131 Napoli, Italy. Fax: +11 39 081 6132229. E-mail: auricchio@tigem.it.*

**Autosomal dominant retinitis pigmentosa caused by the frequent rhodopsin P23H mutation is characterized by progressive photoreceptor cell death eventually leading to blindness and for which no therapies are available. Considering the gain-of-function effect exerted by the P23H mutation, strategies aimed at silencing the expression of the mutated allele, like RNA interference, are desirable. We have designed small interfering RNAs (siRNA) to silence specifically the P23H rhodopsin allele expressed by a transgenic rat model of the disease. We have selected *in vitro* one siRNA and generated an adeno-associated viral (AAV) vector expressing the short hairpin RNA (shRNA) based on the selected siRNA. *In vitro* the shRNA significantly inhibits the expression of the P23H but not the wild-type rhodopsin allele. Subretinal administration of the AAV2/5 vector encoding the shRNA in P23H transgenic rats results in inhibition of rhodopsin P23H expression that is not able to prevent or block photoreceptor degeneration. Since rhodopsin is the most abundant rod photoreceptor protein, systems resulting in more robust shRNA expression in the retina may be required to achieve therapeutic efficacy *in vivo*.**

**Key Words: retinitis pigmentosa, rhodopsin, P23H, photoreceptor cells, RNA interference, AAV**

## INTRODUCTION

Retinitis pigmentosa (RP) includes a large and heterogeneous group of diseases characterized by loss of photoreceptor function and viability [1] and for which no therapies are currently available. RP affects 50,000–100,000 individuals in the United States and 1.5 million worldwide [2]. Clinically, the disease onset includes progressive night blindness, which begins with loss of peripheral vision, evolves to tunnel vision as an effect of rod cell degeneration, and eventually ends in loss of central vision as a consequence of cone cell involvement [1,2]. Fifty percent of nonsyndromic RP cases are sporadic, the remaining are inherited as autosomal dominant, recessive, X-linked, and digenic traits [1,2]. Mutations in more than 80 genes have been associated with RP (www.sph.uth.tmc.edu/Retnet [2]).

Autosomal dominant RP (ADRP) accounts for 40–54% of all RP cases [3]. Rhodopsin mutations are responsible for >25% of ADRP, with more than 150 mutations described, affecting each of the rhodopsin intradiscal, transmembrane, or cytoplasmic domains [1,2,4]. In particular the proline to histidine substitution at codon 23 (P23H) accounts for 12% of all RP cases in the United States [2]. The disease mechanism associated with the P23H mutation remains unclear. Haploinsufficiency is unlikely, since humans and mice heterozygous for rhodopsin null mutations do not show clinical evidence of RP, although they may present with electrophysiological abnormalities [5–8]. In addition transgenic animals overexpressing the P23H allele on a wild-type rhodopsin background present with retinal degeneration [9]. Overexpression of wild-type rhodopsin in P23H transgenic mice slows the progression of retinal degeneration, indirectly suggesting a dominant-



1525-0016/$30.00

negative effect of the mutated allele [10]. Several independent observations point to a gain-of-function effect exerted by the P23H mutation. Overexpression of P23H in cultured cells results in its accumulation in the endoplasmic reticulum (ER) as a consequence of the incorrect folding of the mutated protein [11]. In the ER, misfolded P23H aggregates and overwhelms the proteasome system, leading to cell death [11,12].

Animal models are valuable tools to study *in vivo* the disease pathogenesis and to test experimental therapies. Unfortunately, a mouse model with the knock-in of the human P23H rhodopsin allele has not been generated yet. Transgenic rodents and pigs overexpressing the dominant rhodopsin mutations that recapitulate the human disease have been generated [9,13–16]. Transgenic rats carrying a mutant P23H mouse opsin gene under the transcriptional control of the rhodopsin promoter, which undergo progressive photoreceptor loss, have been developed [14]. Two different lines of P23H rats have been characterized. The line 3 heterozygote transgenic rats carrying one copy of the P23H transgene present with slow photoreceptor degeneration, which at 7 months of age is characterized by a reduction to half of normal of both the outer nuclear layer (ONL) and the electroretinogram (ERG) *b*-wave amplitude [16].

Whether the common P23H mutation exerts a dominant-negative or a gain-of-function effect, therapeutic strategies aiming at inhibiting the expression of the mutated allele rather than supplying a wild-type copy are desirable. Inhibition of gene expression can be achieved by a variety of approaches, including antisense, ribozymes, and, more recently, RNA interference (RNAi) [17]. Allele-specific inhibition of gene expression can be considered for dominant rhodopsin mutations since half dose of the wild-type gene is sufficient for rod function and viability [5,7]. Alternatively, silencing both mutated and wild-type alleles associated with replacement of a wild-type rhodopsin copy resistant to silencing can be envisaged. Unlike the allele-specific approach, this last can be applied to virtually any rhodopsin mutation but requires high efficiency to entirely knock down endogenous rhodopsin expression (which is the most abundant photoreceptor protein [4]) and to obtain rhodopsin gene replacement at appropriate expression levels to be effective avoiding toxicity [10]. Allele-specific inhibition of the P23H rhodopsin has been recently obtained *in vivo* using ribozymes delivered to photoreceptors via adeno-associated viral (AAV) vectors [18,19]. Given the high levels of rhodopsin expression to be silenced [4] and the efficiency of ribozymes, other approaches such as RNAi are being considered. RNAi is performed by short RNA duplexes of 21/23 nucleotides (nt) called small interfering RNAs (siRNAs) that are able to cause degradation of endogenous target messenger RNA (mRNA) recruited by a ribonuclease-containing complex (RNA-induced silencing complex, RISC) [20]. Allele-independent rhodopsin RNAi has been recently obtained *in vitro* [21,22] and its efficacy in the retina has yet to be tested. Recent studies have proved that RNAi can exert robust and specific gene silencing *in vitro* and *in vivo*. In fact, a single mismatch between the target mRNA and its siRNA can completely abrogate silencing [23]. This observation represents the basis for specific RNAi-mediated inactivation of dominant alleles differing from the wild type by one mismatch [24]. The possibility of obtaining RNA interference from duplex or short hairpin RNAs (shRNAs) expressed by viral vectors has enormously enhanced the therapeutic potential of this system, allowing continuous siRNA production, which bypasses the limit of repeated administrations otherwise required to obtain long-term therapeutic effects [25–27]. shRNA processing in target cells results in production of antisense strands complementary to the target mRNA, which lead to its degradation [28]. Vectors derived from the small AAV are among the most efficient and versatile tools to transfer genes to the retina [29]. Exchanging the surface proteins (capsids) among various AAV serotypes allows one to create hybrid AAV vectors (named AAV2/1, 2/2, etc., the first number of which defines the genome and the second the capsid of origin) that have retinal transduction characteristics dependent upon the capsid [30,31]. We and others have demonstrated that vectors with AAV5 capsids (AAV2/5) transfer genes efficiently to the retina of animal models [30–32].

We have designed and tested *in vitro* siRNAs to obtain efficient and preferential silencing of the P23H mutation in the context of a mouse opsin transgene expressed from the rhodopsin promoter in a rat model of the disease. Although this strategy cannot be extrapolated directly to humans considering the nature of the transcript targeted, it can provide an important proof of principle that P23H silencing can be obtained using RNA interference. In addition, since the P23H allele differs by four nucleotides from the endogenous wild-type rat rhodopsin, which is present in two copies in this experimental model, detrimental silencing of wild-type rhodopsin by the shP23H is highly unlikely. Taking advantage of AAV2/5 to transduce rodent photoreceptors efficiently *in vivo*, we expressed shRNA complementary to the P23H mutation in the retina of P23H transgenic rats and describe rhodopsin silencing and its effect on photoreceptor function and morphology in this model.

## Results and Discussion

### *In Vitro* Preferential P23H Rhodopsin RNA Interference

We have designed five 21-nt siRNAs (siRNA0, −1, −2, +1, +2) complementary to the P23H allele expressed in the transgenic rat model. The P23H mismatch with wild-type rhodopsin was placed either in position 18 (siRNA0) or 1 or 2 nucleotides toward the 5′ (siRNA−1, −2) or the 3′ (siRNA+1, +2) end of the oligo. Three additional mis-

doi:10.1016/j.ymthe.2006.07.008

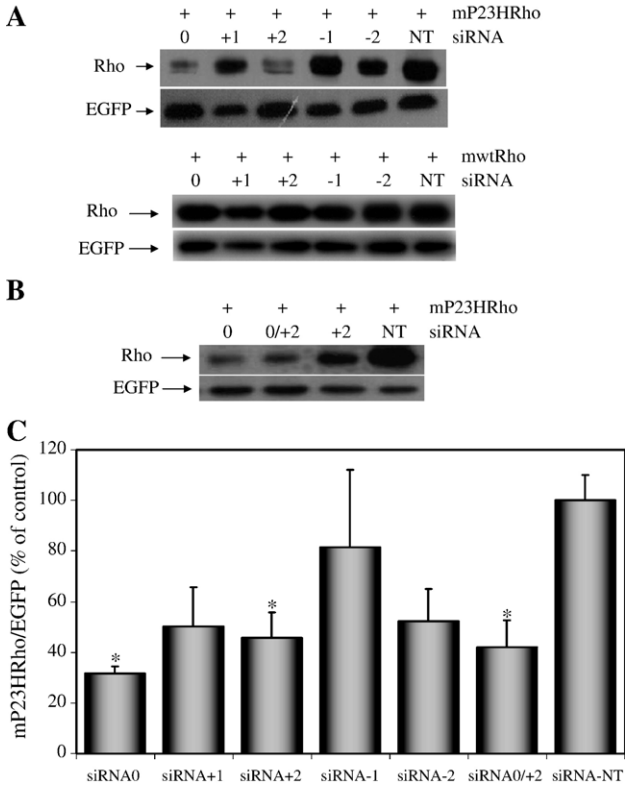


**FIG. 1.** *In vitro* rhodopsin silencing by synthetic siRNAs. (A) Western blot analysis with the anti-rhodopsin 1D4 antibody of total lysates from 293 cells transfected with pAAV-mP23HRho (top) or pAAV-mwtRho (bottom), pAAV-CBA-EGFP, and each of the five siRNAs (siRNA0, −1, −2, +1, +2) as well as a nontargeting siRNA (NTsiRNA). The transfection efficiency was normalized to EGFP expression. (B) Western blot analysis with the anti-rhodopsin 1D4 antibody of total lysates from 293 cells transfected with pAAV-mP23HRho, pAAV-CBA-EGFP, and siRNA0, siRNA+2, the siRNA0/+2 mix, or a nontargeting siRNA (NTsiRNA). The transfection efficiency was normalized to EGFP expression (lower blot). (C) Quantification of the Western blot band intensities. The histograms show the band intensities from four independent experiments as average ± standard error (SE). *$P \leq 0.01$.

matches are present between the mouse and the rat wild-type rhodopsin sequences, thus theoretically avoiding nonspecific silencing by the siRNAs on the wild-type allele. We tested the ability of the designed siRNAs to silence the P23H but not the wild-type allele *in vitro* in 293 cells initially transfected with plasmids expressing either the mouse P23H (mP23HRho) or the wild-type rhodopsin (mwtRho) followed by the independent transfection with each of the five siRNAs selected or with a nontargeting control siRNA (NTsiRNA, against laminin A/C, Fig. 1). We normalized plasmid transfection efficiency by cotransfection with an EGFP-expressing plasmid (pAAV-CBA-EGFP). We harvested the cells, extracted total proteins, and analyzed them by Western blot with anti-rhodopsin antibodies. siRNA0 is the most efficient at silencing mP23HRho synthesis (Fig. 1A). Quantification of rhodopsin protein expression from four independent experiments confirmed that transfection of siRNA0 results in 69 ± 2.7% ($P \leq 0.009$) inhibition of mP23HRho expression (Fig. 1C). Since siRNA + 2 also significantly silences mP23HRho (54.4 ± 10%, $P \leq 0.005$) (Fig. 1C), we tested if the siRNA0 and +2 combination is more efficient at inhibiting mP23HRho expression than siRNA0 alone. Results from four independent experiments showed that there was no synergistic effect between siRNA0 and siRNA + 2 (58.2 ± 10.6% of silencing, $P \leq 0.01$, Figs. 1B and 1C). In addition, none of the five siRNAs tested significantly silenced mwtRho expression in four independent experiments. A representative Western blot analysis of this set of experiments is shown in Fig. 1A, bottom.

To obtain persistent P23H RNA interference, we produced the pAAV-shP23H and -shwt plasmids, which encode shRNAs complementary to either the P23H (shP23H, based on the siRNA0 sequence) or the same region of wild-type (shwt) rhodopsin (Fig. 2A) under the transcriptional control of the Pol II-dependent regulatory

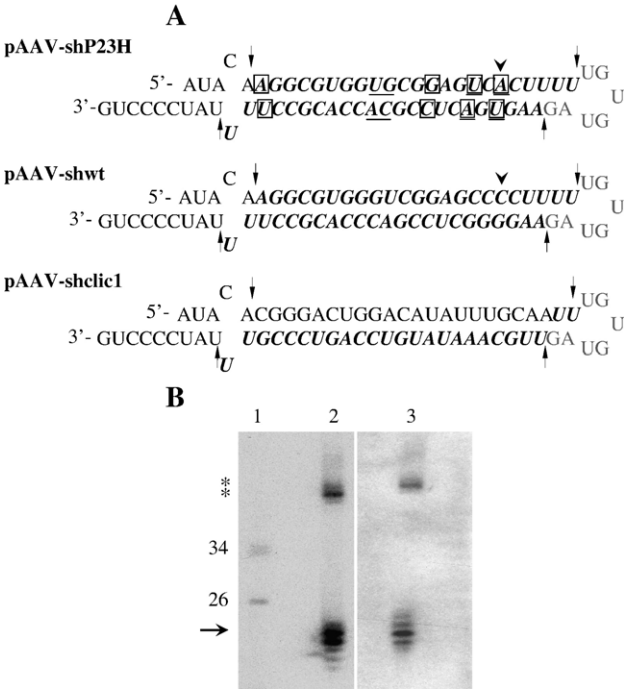


**FIG. 2.** *In vitro* expression of shRNA from pAAV-shwt and -shP23H plasmids. (A) Schematic representation of the short hairpin expressed by the pAAV-shP23H, pAAV-shwt, and pAAV-shclic1 constructs, illustrating the predicted structure of the primary transcripts. The arrows indicate the presumptive sites of processing by the Dicer enzyme. The resulting shRNA sequences are shown in bold. Underlined nucleotides identify the bases that are different between shP23H and shwt and nucleotides in squares are those different from wild-type rat rhodopsin. The P23H mutation is indicated by an arrowhead. (B) Northern blot analysis of total RNA extracted from 293 cells transiently transfected with pAAV-shP23H and pAAV-shwt plasmids. The arrow points at the shP23H (lane 2) and shwt (lane 3) antisense strands. Asterisks indicate the shRNA processing intermediates [33]. A molecular weight marker is loaded in lane 1.

regions of the human U1 small nuclear RNA (snRNA) gene [33]. This is a constitutive and strong promoter that ensures high levels of shRNA expression; in addition, the upstream and downstream sequences flanking the shRNA allow efficient pre-siRNA processing and the specific incorporation of the antisense strand into the RISC [33]. Notably, the U1-expression cassette in the context of an AAV vector has been successfully employed for gene transfer to muscle of therapeutic RNA molecules [34]. The shRNA expression cassette as well as an EGFP expression cassette is inserted in the pAAV-shP23H and-shwt plasmids between the AAV2 ITRs for the following recombinant AAV vector production. We generated a plasmid identical to those described and encoding a nontargeting shRNA (pAAV-shclic1 [35], Fig. 2A) as control. To assess the ability of shP23H and shwt to silence rhodopsin expression, we cotransfected 293 cells with either mP23HRho or mwtRho and with pAAV-shwt or -shP23H. We normalized transfection efficiency by counting cells expressing EGFP from the pAAV-sh plasmids. Forty-eight hours after transfection we extracted RNA and proteins. Northern blot analysis showed abundant production of both shP23H (Fig. 2B, lane 2) and shwt (Fig. 2B, lane 3) antisense strands, while the corresponding sense strands were absent (data not shown). Western blot analysis with anti-rhodopsin antibodies revealed significant and preferential silencing by each shRNA of its complementary allele (Figs. 3A and 3B). As shown in Figs. 3A and 3B, transfection of pAAV-shwt resulted in 86.8 ± 0.88 ($P \leq 0.05$) and 54.3 ± 7.25% ($P \geq 0.1$) reduction in wild-type and P23H rhodopsin, respectively. Transfection of pAAV-shP23H, instead, reduced by 63.8 ± 12.1 ($P \leq 0.02$) and 11.7 ± 16% ($P \geq 0.4$) the levels of P23H and wild-type rhodopsin, respectively (Figs. 3A and 3B). Real-time PCR analysis of rhodopsin messenger RNA from the same samples confirmed the effect observed at the protein level: transfection of pAAV-shwt resulted in 66.6 ± 11.6 ($P \leq 0.04$) and 33.1 ± 19.17% ($P \geq 0.2$) reduction of mwtRho and mP23HRho RNA, respectively; transfection of pAAV-shP23H resulted in 65.1 ± 4.9% ($P \leq 0.02$) silencing of mP23HRho RNA, while it did not affect the levels of mwtRho (Fig. 3C). Both the Western blot and the PCR results are the averages of four independent experiments. These results support a significant silencing effect of each shRNA that is specific for the complementary rhodopsin allele.

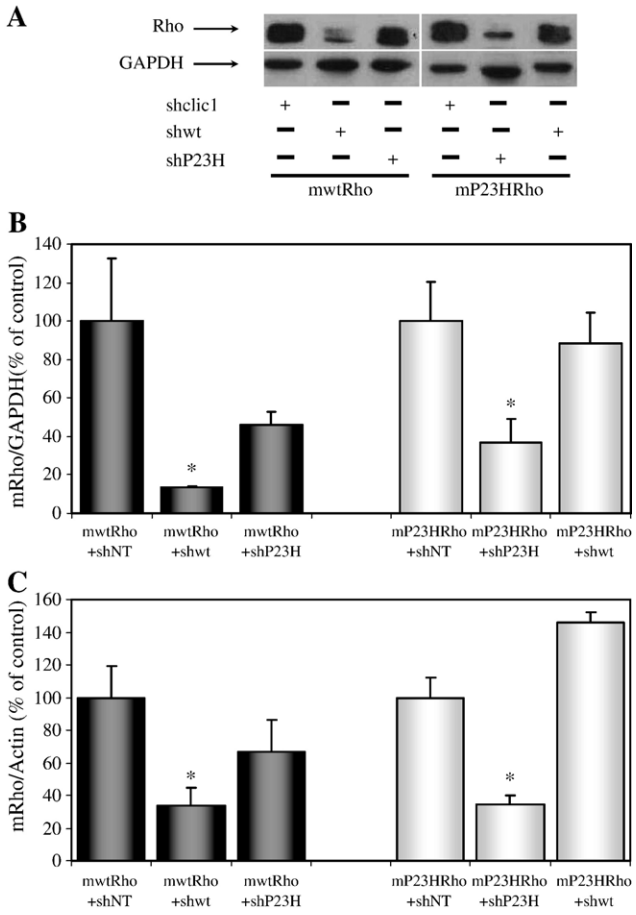


**FIG. 3.** Allele-preferential rhodopsin silencing by shRNAs. (A) Western blot with either anti-rhodopsin (top) or anti-GAPDH (bottom) antibodies of total lysates from 293 cells cotransfected with either pAAV-mwtRho or pAAV-mP23HRho and with pAAV-shclic1 (shclic1), pAAV-shwt (shwt), or pAAV-shP23H (shP23H). Arrows point at the rhodopsin (Rho) or GAPDH bands. (B) Quantification of Western blot band intensities *$P \leq 0.05$. (C) Real-time PCR analysis of mRNA from the same samples as in B. *$P \leq 0.04$. The results are the averages of four independent experiments.

**Rhodopsin RNA Interference in the Retina of P23H Transgenic Rats Transduced with AAV2/5 Vectors**

We used the pAAV-shP23H and -shwt plasmids to produce recombinant AAV2/5 vectors. We injected AAV2/5-shP23H subretinally ($2.4 \times 10^{10}$ genome copies (GC)/eye) in one eye of 21-day-old transgenic P23H rats ($n = 6$) and injected the contralateral eye with the same dose of AAV2/5-shwt. As an additional experimental control, we injected two animals with the same dose of AAV2/5-CMV-EGFP in both eyes. Three/four weeks later we sacrificed animals and isolated retinas for RNA extraction. We performed Northern blot on retinas from two animals, showing an evident expression of the antisense P23H strand in the retinas transduced with the AAV2/5-shP23H vectors (Fig. 4A). These data demonstrate that the shRNAs are stably expressed from the U1 promoter and that their processing to antisense strands occurs correctly in the retina. The different levels of the P23H antisense strands detected in the two retinas analyzed suggest the presence of variability presumably due to vector delivery in these two cases. We used the remaining four animals for the assessment of inhibition of P23H rhodopsin expression following AAV-mediated gene transfer. We performed one-step real-time PCR analysis on mRNA from each retina separately ($n = 4$

doi:10.1016/j.ymthe.2006.07.008

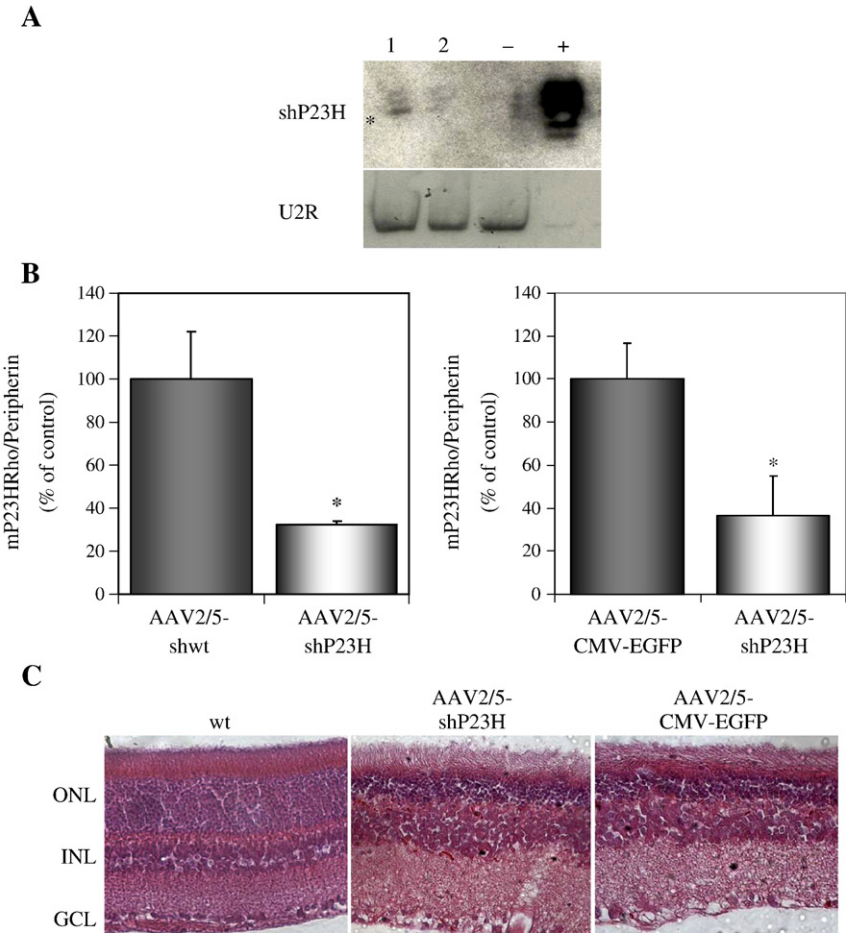


**FIG. 4.** AAV-mediated shRNA expression in transgenic P23H rat retinas results in significant rhodopsin P23H silencing but does not inhibit retinal degeneration. (A) Northern blot analysis of total RNA isolated from retinas of animals injected with either AAV2/5-shP23H (lanes 1 and 2) or AAV2/5-CMV-EGFP (lane –). Lane + contains RNA from pAAV-shP23H-transfected 293 cells as control. The top shows the Northern blot hybridized with a shP23H-specific probe, while the bottom shows the hybridization with the probe for the ubiquitous U2 small nuclear RNA. (B) Left: Real-time PCR of mRNAs from retinas of P23H transgenic rats subretinally injected with either AAV2/5-shP23H or AAV2/5-shwt. The histogram shows the average ± SE. $*P \leq 0.04$. Right: Real-time PCR of mRNAs from retinas of P23H transgenic rats subretinally injected with either AAV2/5-shP23H or AAV2/5-EGFP. The histogram shows the average ± SE. $*P \leq 0.05$ (C) Histological analysis of wild-type (wt) or mP23H transgenic rat retinas injected with either AAV2/5-shP23H or AAV2/5-CMV-EGFP. The sections were stained using hematoxylin and eosin. ONL, outer nuclear layer; INL, inner nuclear layer; GCL, ganglion cell layer.

eyes/group), using a set of primers/probe specific for the mouse rhodopsin transgene (mP23HRho). We normalized levels of mP23HRho to those of rat peripherin, an endogenous photoreceptor-specific protein, which should not be affected by shRNA expression. A 68 ± 1.9% ($P \leq 0.04$) mP23HRho decrease in levels was observed in AAV2/5-shP23H-injected eyes compared to the contralateral AAV2/5-shwt-treated eyes (Fig. 4B, graph on the left). The levels of mP23HRho silencing correlate with the levels of retinal transduction (30–50%) observed following a single subretinal injection of AAV. In addition, the AAV2/5-shwt administration did not alter the mP23HRho levels as it resulted from the comparison with the AAV2/5-CMV-EGFP-injected retinas ($n = 4$, data not shown).

We injected an additional group of 16 transgenic P23H rats (21 days of age) with AAV2/5-shP23H in one eye and with AAV2/5-CMV-EGFP in the contralateral eye, to evaluate the impact of silencing on retinal structure and function following AAV-mediated gene transfer. We performed Ganzfeld flash ERGs under scotopic and photopic conditions on all animals at 4 and 7 months of age, when the animals were sacrificed and their eyes enucleated and partly embedded and sectioned for histological analysis, partly used for isolation of RNA and proteins from whole retinas. We performed one-step real-time PCR analysis specific for mP23HRho on mRNA from each retina separately ($n = 4$ eyes/group) and normalized it to rat peripherin, as described above. We observed a decrease in the levels of mP23HRho to 57.6, 16.4, 34.2, and 46.5% (average 38.7 ± 8.82%, $P \leq 0.05$) of the contralateral EGFP-treated eyes for each eye injected with the shRNA-expressing vector (Fig. 4B, graph on right). This perfectly agrees with the data collected on the animals injected with AAV2/5 and sacrificed 3 weeks after subretinal injection. This confirms that silencing is sustained from 3 weeks to 7 months after AAV subretinal injection and that both administrations of AAV2/5-shwt and-CMV-EGFP do not impact on mP23HRho levels. We performed Western blot analysis of protein extracts from the same retinas used for RNA analyses using the anti-rhodopsin 1D4 antibody, which cross-reacts with both rat and mouse (mP23HRho) rhodopsin expressed by the transgenic P23H animals. We observed no significant

differences at this level between AAV2/5-shP23H-and AAV2/5-CMV-EGFP-injected eyes (data not shown), suggesting that the mP23HRho silencing effect detected at the mRNA level is masked at the protein level by the abundance of the endogenous rat rhodopsin, which differs by four nucleotides from the shP23H (Fig. 2A) and is therefore not silenced.

To test if the reduction in the mP23HRho mRNA levels detected in the AAV2/5-shP23H injected eyes impacts on photoreceptor structure and number, we analyzed eyes from nine animals at the histological level. The number of rows of photoreceptor nuclei counted on the nasal, temporal (injected), and central sides of the retinas was not significantly different between eyes injected with AAV2/5-shP23H (average: 4.17 ± 1.1) and those injected with AAV2/5-CMV-EGFP (average: 4.4 ± 1.2). Representative pictures of sections from AAV-treated and control retinas are shown in Fig. 4C. The Ganzfeld flash ERGs recorded at 4 and 7 months of age did not show significant differences between AAV2/5-shP23H-and AAV2/5-CMV-EGFP-treated eyes, as evidenced by the *b*-wave amplitude in both sets of eyes. The mean amplitude of *b*-wave recorded in 4-month-old animals under scotopic conditions (stimulus intensity: 20 cd m−2) was 393.5 ± 25.6 and 362.9 ± 30.9 μV in the AAV2/5-shP23H and in the AAV2/5-CMV-EGFP injected eyes, respectively. The analysis performed at 7 months of age evidenced *b*-wave amplitudes of 19.4 ± 6.3 and 16.6 ± 4.2 μV in the AAV2/5-shP23H-and in the AAV2/5-CMV-EGFP-treated eyes, respectively ($n$ = 16 eyes/group). We selected the two time points for the ERG analysis because of: (1) the progress of retinal degeneration in the animals [16], (2) the levels of retinal transduction obtained after a single subretinal AAV administration, and (3) the non-cell-autonomous mechanism of photoreceptor degeneration. Therefore, an earlier time point would allow one to assess efficacy, which could be transient should the levels of P23H silencing be partial or the loss of untransduced photoreceptor influence the survival of those transduced by AAV. The absence of a functional rescue at 4 months of age argues against the possibility that a transient AAV2/5-shP23H protective effect present initially is then lost over time at 7 months of age, the endpoint of the study.

In conclusion, we have designed an allele-dependent RNAi approach for the P23H dominant mutation in the context of a mouse opsin transgene overexpressed in a rat model of the disease. We have obtained preferential and partial mRNA and protein P23H knockdown *in vitro* using synthetic siRNAs as well as shRNAs expressed from plasmids. *In vivo*, we have obtained shRNA expression in the rat retina transduced with AAV2/5 vectors resulting in reduction of rhodopsin P23H mRNA levels to 38.7%, which was not sufficient to inhibit neither at the functional nor at the morphological level the photoreceptor degeneration present in the P23H rats. This is not surprising since rhodopsin is the most abundant photoreceptor protein [4], which is continuously produced as result of photoreceptor outer segment phagocytosis by retinal pigment epithelium. In addition, the minimal P23H levels causing photoreceptor degeneration are unknown. Our data suggest that the 38.7% of mP23HRho levels remaining after silencing still result in significant photoreceptor degeneration. It is possible that systems resulting in higher levels of shRNA production in photoreceptors than the AAV vector or the U1 snRNA promoter we used may achieve levels of P23H silencing able to slow or block photoreceptor apoptosis in the P23H transgenic rats. Alternatively, a mutation-independent siRNA strategy coupled to gene replacement may result in higher levels of silencing than those obtained with the mutation-dependent approach we described here. Indeed in the former case there is no positional constraint for the selection of the most potent siRNA. Ultimately, strategies to silence rhodopsin expression acting *in cis*, i.e., at the level of the promoter, which is present in two copies/diploid genome, may overcome the limit represented by the high levels of rhodopsin expression in photoreceptors. This has to be coupled (as in the case of mutation-independent silencing) to replacement with the wild-type rhodopsin cDNA under the control of a promoter resistant to the silencing construct. The recent development of zinc-finger technologies for *in vivo* modulation of gene expression [36] may allow the success of such silencing strategy.

## Materials and Methods

***Generation of the plasmid constructs.*** The murine wild-type rhodopsin coding sequence was amplified from mouse retina cDNA, while the P23H rhodopsin was obtained from the P23H transgenic rat genomic DNA. In both cases, PCR was performed using the Advantage cDNA PCR Kit (Clontech, Palo Alto, CA, USA) to insert a *Not*I and a *Hin*dIII site at the 5′ and 3′ end, respectively with the following primers: mRho-NotI-F, 5′-GCGGCCGCATGAACGGCACAGAGGGCC-3′, and mRho-HindIII-R, 5′-AAGCTTTTAGGCTGGAGCCACCTGG-3′. The PCR products were then digested with *Not*I and *Hin*dIII and cloned into pAAV2.1-CMV-EGFP [30] by removing the EGFP coding sequence (*Not*I–*Hin*dIII) to obtain pAAV2.1-CMV-mwtRho and pAAV2.1-CMV-mP23HRho, respectively.

The sequences utilized in the three different constructs, pAAV-shP23H, pAAV-shwt, and pAAV-shclic1b (as a nontargeting control against clic1, a gene not expressed in CNS neurons [35]) are shown in Fig. 2A and were generated by annealing corresponding complementary synthetic oligonucleotides, as described in [33], which were then cloned into the *Bgl*II–*Xho*I sites of vector pSiUx [33]. To generate the pAAV derivatives, the transcriptional unit was excised with *Xba*I and *Nhe*I and cloned into the *Nhe*I site of the pAAV2.1-CMV-EGFP plasmid. Therefore, all these constructs express EGFP. The pAAV-CBA-EGFP plasmid was kindly provided by Drs. Chiara Abrescia and Enrico M. Surace (Telethon Institute of Genetics and Medicine (TIGEM), Naples, Italy).

***AAV vector production and purification.*** AAV vectors were produced by the TIGEM AAV Vector Core using pAAV2.1-shP23H and pAAV2.1-CMV-EGFP [30]. Recombinant AAV5 viruses were produced by triple transfection of 293 cells followed by $CsCl_2$ purification of the vectors as previously described [30]. For each viral preparation, physical titers (GC/ml) were determined by both PCR quantification using TaqMan (Perkin–Elmer, Life and Analytical Sciences, Inc.) [37] and dot-blot analysis.

doi:10.1016/j.ymthe.2006.07.008

***siRNA design and in vitro selection.*** The five 21-nt sequences (AGGCGUGGUGCGGAGUCACUU (siRNA0), CAGGCGUGGUGCGGAGUCACU (siRNA−1), ACAGGCGUGGUGCGGAGUCAC (siRNA−2), GGCGUGGUGCGGAGUCACUUC (siRNA + 1), GCGUGGUGCGGAGUCACUUCG (siRNA + 2)) and a nontargeting siRNA (against laminin A/C, NT-siRNA) were synthesized by Dharmacon RNA Technologies (Lafayette, CO, USA). Alignment of the siRNAs with accessible mammalian sequences via the NCBI BLAST program did not reveal identity with genes other than rhodopsin or laminin as expected. 293 cells were plated in six-well plates to a concentration of 3 × 105 cells/well. Twenty-four hours later, the cells were cotransfected using FUGENE 6 (Roche, Basel, Switzerland) according to the manufacturer's instruction with a mix of two plasmids: 1 μg of pAAV2.1-CMV-mwtRho or pAAV2.1-CMV-mP23HRho and 1 μg of pAAV2.1-CBA-EGFP per well. Twenty-four hours after this first transfection, cells were rinsed and transfected again with 5 μg of each of the five siRNAs using Lipofectamine 2000 as suggested by the manufacturer (Gibco BRL–Invitrogen, Life Technologies, Gaithersburg, MD, USA) in a total volume of 1 ml per well.

The two plasmids pAAV-shwt and pAAV-shP23H were cotransfected with either pAAV-mwtRho or pAAV-mP23HRho using FUGENE 6 (Roche, Basel, Switzerland) in 293 cells plated in six-well plates as described above, to test shRNA efficiency.

***RNA extraction and analysis.*** Total RNA and poly(A)$^+$ RNA were isolated from transfected 293 cells using the TRIzol Reagent (Invitrogen) and the Oligotex mRNA purification kit (Qiagen S.p.A., Milan, Italy). cDNAs were amplified using the Qiagen QuantiTech reverse transcription kit, according to the manufacturer's instructions. Real-time PCR analysis was performed on mRNA to analyze the mP23HRho transcript and on cDNA to analyze the peripherin transcript. All primers/probes chosen for the genes met the established criteria for TaqMan probes (PE Biosystems, Foster City, CA, USA). The mRho probe (5′-CAGCTTGACAAAGGGCATCCATCCA-3′) had a melting temperature of 69°C and was synthesized using PE Applied Biosystems technology, labeled with 6-carboxy fluorescein at the 5′ end and 6-carboxy tetramethyl rhodamine (TAMRA) at the 3′ end. All reactions (50 μl) were performed with 20 ng mRNA, 25-μl Master Mix Reagent Kit (Applied Biosystems), 120 pmol TaqMan probe, and 10 μM specific primers. The following amplification conditions were used: 10 min at 25°C, 30 min at 48°C, and 10 min at 95°C. These conditions were followed by 40 cycles of denaturation for 15 s at 95°C and annealing for 1 min at 60°C. The peripherin primers used were PerF, 5′-GAACATCGCGGCGAAGAAT-3′, and PerR, 5′-CATCGGACAGGTCAGCGTATT-3′. The PCRs with cDNA were carried in 25 μl total volume using 12.5 μl SYBR Green Master Mix (Applied Biosystems) and 400 nM primer under the following conditions: preheating, 50°C for 2 min and 95°C for 10 min; cycling, 40 cycles of 95°C for 15 s and 60°C for 1 min. All the reactions were standardized against GAPDH by using specific primers/probes (Applied Biosystems) labeled with VIC at the 5′ end and with TAMRA at the 3′ end. All the RT reactions were performed by using an iCycler iQ multicolor real-time detection system (Bio-Rad, Hercules, CA, USA) equipped with a 96-well thermal cycler.

To detect siRNAs using Northern blot analysis, total RNA from transiently transfected 293 cells (3 μg) or from retinas of injected animals (30 μg) was separated on a 10% polyacrylamide–8 M urea gel and transferred by electroblotting onto Hybond-N$^+$ membrane (Amersham Pharmacia Biotech, Milan, Italy). The hybridization was carried out at 37°C in 5 × SSPE1, × Denhardt's solution, 0.5% SDS, 25 μg/ml salmon sperm DNA (Invitrogen). Washes were performed at 37°C in 6 × SSPE, 2 × SSPE, and finally 0.2 × SSPE. Probes used were terminally $^{32}$P-radiolabeled DNA oligos: senP23H (5′-GGCGTGGTGCGGAGTCACTT-3′), antiP23H (5′-AAGTGACTCCGCACCACGCC-3′); senwtRho (5′-GGCGTGGGTCGGAGCCCCTT-3′), and antiwtRho (5′-AAGGGGCTCCGACCCACGCC-3′). The endogenous U2 snRNA was detected with probe U2R [38]. Filters were exposed on BioMax MS film (Kodak) for 5 h at −180°C with a BioMax MS intensifying screen (Kodak).

***Protein extraction and Western blot analysis.*** Transfected 293 cells were homogenized in TRIzol Reagent (Invitrogen) and total proteins were extracted according to the manufacturer's instruction. Total proteins were measured using the BCA protein assay reagent (Pierce Chemical Co., Boston, MA, USA). Proteins were separated by SDS–PAGE (10% gel) under reducing conditions and transferred to a PVD membrane (Millipore, Billerica, MA, USA). Membranes were incubated overnight in blocking buffer and subsequently probed with the specific antibodies [anti-rhodopsin 1D4 antibody (a kind gift from Dr. Valeria Marigo, TIGEM, Naples, Italy, produced by the National Cell Culture Center) and anti-EGFP antibody (Santa Cruz Biotechnology, Santa Cruz, CA, USA)] for 3 h at room temperature. Anti-GAPDH (Abcam, Cambridge, MA, USA) was used as loading control. The blots were developed using the Enhanced Chemiluminescence Kit (Pierce Chemical Co.). The Western blot bands were quantified using the Image Processing Tool Kit v.5 Plus (Fovea Pro 3.0, Asheville, NC, USA).

***Animal model, vector administration, and tissue collection.*** All procedures were performed in accordance with institutional guidelines for animal research. P23H homozygous animals for breeding were kindly provided by Matthew M. LaVail, Ph.D. (Backman Vision Center, USCF School of Medicine, University of California at San Francisco) and were bred in the animal house of the Biotechnology Center of the Cardarelli Hospital (Naples, Italy) against albino Sprague–Dawley rats (Harlan, Indianapolis, IN, USA) to obtain P23H heterozygous rats, bringing a single copy of the P23H transgenic allele in addition to the two normal copies of the wild-type rhodopsin alleles. The generation of the mouse opsin transgene have been obtained incorporating the following modifications: GT to TG at codon 20, which generates an amino acid polymorphism (Val to Gly); C to T modification at position 1499, which would not change the amino acid sequence; and C to A change to create the P23H mutation at codon 23 and A to T at position 1536, which will not change the amino acid sequence [16].

At P21, animals were anesthetized on ice and subretinally injected in the right eye with 4 μl of AAV2/5-U1-shP23H vector ($6.3 \times 10^{12}$ GC/ml) and the same dose of AAV2/5-shwt or AAV2/5-CMV-EGFP in the left eye, as control. Subretinal vector administration was performed as described [39]. Rats were sacrificed at 3 weeks or at 7 months of age. For immunohistochemistry, eyecups were harvested, fixed by immersion in 4% paraformaldehyde, and embedded in paraffin and sequential 5-μm coronal sections were cut. For RNA or protein extractions, the isolated retinas were removed and snap-frozen in liquid nitrogen and treated as described in the above sections (RNA extraction and analysis and Protein extraction and Western blot analysis).

***Histological analysis.*** For each eye 150 to 200 serial sections (5 μm thick) were cut along the horizontal meridian; the sections were progressively distributed on 10 slides so that each slide contained 15 to 20 sections representative of the whole eye at different levels. The sections were stained with hematoxylin and eosin (Richard-Allen Scientific, Kalamazoo, MI, USA; Aldrich, Milan, Italy) and retinal histology was analyzed by light microscopy. To quantify photoreceptor rescue, the number of nuclei in the ONL of each eye was counted. For each section, the number of nuclei in the ONL was separately counted on the nasal, central, and temporal sides. The nasal, temporal, and central counts of each section were independently averaged, therefore obtaining a number that was the average of the three sides for each eye. The counts from each group (right and left eyes) were then averaged and standard deviations were calculated. *P* values were calculated using Student's *t* test.

***Electroretinogram measurements.*** ERGs were performed on 4-and 7-month-old rats as previously described [40,41]. Briefly, animals were dark adapted for 3 h and then anesthetized and accommodated in a stereotaxic apparatus under dim red light. ERGs were evoked by flashes of different light intensities ranging from $10^{-4}$ to 20 cd m$^{-2}$ s$^{-1}$ generated through a Ganzfeld stimulator (Lace). To minimize the noise, three different responses evoked by light were averaged for each luminance step. The electrophysiological signals were recorded throughout gold plate electrodes inserted under the lower eyelids. Electrodes in each eye were referred to a needle electrode inserted subcutaneously at the level of the corresponding frontal region. The different electrodes were connected to a two-channel amplifier. Amplitudes of *a*-and *b*-waves were plotted as a

function of increasing light intensities. After completion of responses obtained under dark-adapted conditions the recording session continued with the aim to dissect the cone pathway mediating the light response. To this aim the ERG in response to light of 20 cd $m^{-2}$ was recorded in the presence of a continuous background light (background light set at 15 cd $m^{-2}$). The amplitude of the *b*-wave for each eye was plotted as a function of luminance (transfer curve) under scotopic and photopic conditions. For each group the mean *b*-wave amplitude was plotted.

## ACKNOWLEDGMENTS

*We thank Graciana Diez Roux for critical reading of the manuscript and Armida Faella for experimental help in the revised version of the work. This work was supported by Telethon Grant TIGEM P04, the Milton & Steinbach Fund, EC-FP6 Projects LSHB-CT-2005-512146 "DiMI" and 018933 "Clinigene," NIH 1R01EY015136-01, and Grant D.M.589/7303/04 from the Italian Ministry of Agriculture. The work of I.B. was supported by the Sixth Research Framework Programme of the European Union, Project RIGHT (LSHB-CT-2004 005276), the PRIN, and the "Centro di Eccellenza BEMM."*

RECEIVED FOR PUBLICATION MARCH 16, 2006; REVISED JULY 17, 2006; ACCEPTED JULY 17, 2006.

## REFERENCES

1. Dryja, T. (2001). Retinitis pigmentosa and stationary night blindness. In: *The Metabolic & Molecular Bases of Inherited Diseases,* 8th ed. (C. Scriver, A. Beaudet, W. Sly, and D. Valle, Eds.). McGraw–Hill, New York.
2. Wang, D. Y., *et al.* (2005). Gene mutations in retinitis pigmentosa and their clinical implications. *Clin. Chim. Acta* **351:** 5 – 16.
3. Wilson, J. H., and Wensel, T. G. (2003). The nature of dominant mutations of rhodopsin and implications for gene therapy. *Mol. Neurobiol.* **28:** 149 – 158.
4. Kisselev, O. G. (2005). Focus on molecules: rhodopsin. *Exp. Eye Res.* **81:** 366 – 367.
5. Rosenfeld, P. J., *et al.* (1992). A null mutation in the rhodopsin gene causes rod photoreceptor dysfunction and autosomal recessive retinitis pigmentosa. *Nat. Genet.* **1:** 209 – 213.
6. Rosenfeld, P. J., Hahn, L. B., Sandberg, M. A., Dryja, T. P., and Berson, E. L. (1995). Low incidence of retinitis pigmentosa among heterozygous carriers of a specific rhodopsin splice site mutation. *Invest. Ophthalmol. Visual Sci.* **36:** 2186 – 2192.
7. Humphries, M. M., *et al.* (1997). Retinopathy induced in mice by targeted disruption of the rhodopsin gene. *Nat. Genet.* **15:** 216 – 219.
8. Greenberg, J., Roberts, L., and Ramesar, R. (2003). A rare homozygous rhodopsin splice-site mutation: the issue of when and whether to offer presymptomatic testing. *Ophthalmic Genet.* **24:** 225 – 232.
9. Olsson, J. E., *et al.* (1992). Transgenic mice with a rhodopsin mutation (Pro23His): a mouse model of autosomal dominant retinitis pigmentosa. *Neuron* **9:** 815 – 830.
10. Tan, E., *et al.* (2001). The relationship between opsin overexpression and photoreceptor degeneration. *Invest. Ophthalmol. Visual Sci.* **42:** 589 – 600.
11. Saliba, R. S., Munro, P. M., Luthert, P. J., and Cheetham, M. E. (2002). The cellular fate of mutant rhodopsin: quality control, degradation and aggresome formation. *J. Cell Sci.* **115**(Pt 14)**:** 2907 – 2918.
12. Illing, M. E., Rajan, R. S., Bence, N. F., and Kopito, R. R. (2002). A rhodopsin mutant linked to autosomal dominant retinitis pigmentosa is prone to aggregate and interacts with the ubiquitin proteasome system. *J. Biol. Chem.* **277:** 34150 – 34160.
13. Naash, M. I., Hollyfield, J. G., al-Ubaidi, M. R., and Baehr, W. (1993). Simulation of human autosomal dominant retinitis pigmentosa in transgenic mice expressing a mutated murine opsin gene. *Proc. Natl. Acad. Sci. USA* **90:** 5499 – 5503.
14. Steinberg, R., *et al.* (1996). Transgenic rat models of inherited retinal degeneration caused by mutant opsin genes. *Invest. Ophthalmol. Visual Sci.* **37**(Suppl.)**:** S698. [ARVO Abstract No. 3190].
15. Petters, R. M., *et al.* (1997). Genetically engineered large animal model for studying cone photoreceptor survival and degeneration in retinitis pigmentosa. *Nat. Biotechnol.* **15:** 965 – 970.
16. Machida, S., *et al.* (2000). P23H rhodopsin transgenic rat: correlation of retinal function with histopathology. *Invest. Ophthalmol. Visual Sci.* **41:** 3200 – 3209.
17. Sioud, M., and Iversen, P. O. (2005). Ribozymes, DNAzymes and small interfering RNAs as therapeutics. *Curr. Drug Targets* **6:** 647 – 653.
18. Lewin, A. S., *et al.* (1998). Ribozyme rescue of photoreceptor cells in a transgenic rat model of autosomal dominant retinitis pigmentosa. *Nat. Med.* **4:** 967 – 971.
19. LaVail, M. M., *et al.* (2000). Ribozyme rescue of photoreceptor cells in P23H transgenic rats: long-term survival and late-stage therapy. *Proc. Natl. Acad. Sci. USA* **97:** 11488 – 11493.
20. Hutvagner, G. (2005). Small RNA asymmetry in RNAi: function in RISC assembly and gene regulation. *FEBS Lett.* **579:** 5850 – 5857.
21. Cashman, S. M., Binkley, E. A., and Kumar-Singh, R. (2005). Towards mutation-independent silencing of genes involved in retinal degeneration by RNA interference. *Gene Ther.* **12:** 1223 – 1228.
22. Kiang, A. S., *et al.* (2005). Toward a gene therapy for dominant disease: validation of an RNA interference-based mutation-independent approach. *Mol. Ther.* **12:** 555 – 561.
23. Hamada, M., *et al.* (2002). Effects on RNA interference in gene expression (RNAi) in cultured mammalian cells of mismatches and the introduction of chemical modifications at the 3′-ends of siRNAs. *Antisense Nucleic Acid Drug Dev.* **12:** 301 – 309.
24. Rodriguez-Lebron, E., and Paulson, H. L. (2006). Allele-specific RNA interference for neurological disease. *Gene Ther.* **13:** 576 – 581.
25. Brummelkamp, T. R., Bernards, R., and Agami, R. (2002). Stable suppression of tumorigenicity by virus-mediated RNA interference. *Cancer Cell* **2:** 243 – 247.
26. Rubinson, D. A., *et al.* (2003). A lentivirus-based system to functionally silence genes in primary mammalian cells, stem cells and transgenic mice by RNA interference. *Nat. Genet.* **33:** 401 – 406.
27. Xia, H., *et al.* (2004). RNAi suppresses polyglutamine-induced neurodegeneration in a model of spinocerebellar ataxia. *Nat. Med.* **10:** 816 – 820.
28. Amarzguioui, M., Rossi, J. J., and Kim, D. (2005). Approaches for chemically synthesized siRNA and vector-mediated RNAi. *FEBS Lett.* **579:** 5974 – 5981.
29. Auricchio, A., and Rolling, F. (2005). Adeno-associated viral vectors for retinal gene transfer and treatment of retinal diseases. *Curr. Gene Ther.* **5:** 339 – 348.
30. Auricchio, A., *et al.* (2001). Exchange of surface proteins impacts on viral vector cellular specificity and transduction characteristics: the retina as a model. *Hum. Mol. Genet.* **10:** 3075 – 3081.
31. Yang, G. S., *et al.* (2002). Virus-mediated transduction of murine retina with adeno-associated virus: effects of viral capsid and genome size. *J. Virol.* **76:** 7651 – 7660.
32. Pawlyk, B. S., *et al.* (2005). Gene replacement therapy rescues photoreceptor degeneration in a murine model of Leber congenital amaurosis lacking RPGRIP. *Invest. Ophthalmol. Visual Sci.* **46:** 3039 – 3045.
33. Denti, M. A., Rosa, A., Sthandier, O., De Angelis, F. G., and Bozzoni, I. (2004). A new vector, based on the PolII promoter of the U1 snRNA gene, for the expression of siRNAs in mammalian cells. *Mol. Ther.* **10:** 191 – 199.
34. Denti, M. A., *et al.* (2006). Body-wide gene therapy of Duchenne muscular dystrophy in the *mdx* mouse model. *Proc. Natl. Acad. Sci. USA* **103:** 3758 – 3763.
35. Novarino, G., *et al.* (2004). Involvement of the intracellular ion channel CLIC1 in microglia-mediated beta-amyloid-induced neurotoxicity. *J. Neurosci.* **24:** 5322 – 5330.
36. Park, K. S., *et al.* (2003). Phenotypic alteration of eukaryotic cells using randomized libraries of artificial transcription factors. *Nat. Biotechnol.* **21:** 1208 – 1214.
37. Gao, G., *et al.* (2000). Purification of recombinant adeno-associated virus vectors by column chromatography and its performance in vivo. *Hum. Gene Ther.* **11:** 2079 – 2091.
38. De Angelis, F. G., *et al.* (2002). Chimeric snRNA molecules carrying antisense sequences against the splice junctions of exon 51 of the dystrophin pre-mRNA induce exon skipping and restoration of a dystrophin synthesis in Delta 48–50 DMD cells. *Proc. Natl. Acad. Sci. USA* **99:** 9456 – 9461.
39. Liang, F. Q., Anand, V., Maguire, A., and Bennett, J. (2000). Intraocular delivery of recombinant virus. *Methods Mol. Med.* **47:** 125 – 139.
40. Domenici, L., Berardi, N., Carmignoto, G., Vantini, G., and Maffei, L. (1991). Nerve growth factor prevents the amblyopic effects of monocular deprivation. *Proc. Natl. Acad. Sci. USA* **88:** 8811 – 8815.
41. Lyubarsky, A. L., *et al.* (2002). Functionally rodless mice: transgenic models for the investigation of cone function in retinal disease and therapy. *Vision Res.* **42:** 401 – 415.